Organic Process Research & Development

Article

pubs.acs.org/OPRD

Application-Oriented Analysis of Mixing Performance in Microreactors

Sebastian Schwolow,[†] Jutta Hollmann,[‡] Berthold Schenkel,[‡] and Thorsten Röder*[,†]

[†]Institut für Chemische Verfahrenstechnik, Hochschule Mannheim, Paul-Wittsack-Straße 10, 68163 Mannheim, Germany

[‡]Novartis Pharma AG, Lichtstrasse 35, 4056 Basel, Switzerland

ABSTRACT: A methodology was developed to select adequate, commercially available micromixers for mixing sensitive chemical reactions. The range of flow rates can be derived at which the selected micromixers have to be operated to ensure the required mixing intensity. This methodology enables the selection of adequate micromixers for the scale up of the chemical reactions to higher flow rates. Two chemical test reactions were used for an experimental approach to characterize the selected microreactors. Both reactions are based on the effect of micromixing on the product distribution of competitive reaction systems. Flow rates and pressure drop were determined at which the mixing times are short relative to the reaction times. In this case, influences of mixing on the selectivity of the reference reaction can be neglected. Since two reference reactions with different time scales for mixing and reaction were tested, it was possible to study the mixing performance of a variety of micromixers over a wide range of flow rates. The investigated micromixers differ in their dimensions, internal geometry, and mixing principle. In the present work, overview tables are provided as a tool to evaluate the commercially available micromixers for specific applications. Further, the influence of mixing principle and pressure drop is discussed.

INTRODUCTION

In the past few years, the use of micromixers has gained increasing significance for various applications in chemistry. The main advantage of microstructured reactors is the enhancement of heat and mass transfer due to the high surface-to-volume ratio and the increased intensity of fluid mixing.

The fast development in microreaction technology has led to a high number of available micromixers, based on entirely different mixing principles.[1] Thus, the choice of a commercially available mixer as well as the design of new devices for a particular application can be difficult. Complex interactions of fluid mechanics, mass transfer, and reactions have to be considered. For an efficient reactor selection, optimized for specific reactions, experimental investigations of mixing processes are necessary.

The main objective of this work is the characterization of several commercially available, passive micromixers to provide assistance for the selection and scale-up of microreaction devices. Due to the complex nature of mixing processes and the variety of applied mixing principles, an experimental approach was taken. It is focusing on the interactions between mixing and chemical reactions. The degree to which the chemical reactions are determined by the mixing process is mainly influenced by the ratio of the characteristic times for mixing and reaction. If the mixing time is significantly shorter than the reaction time, it can be assumed that the reaction takes place in a homogeneous concentration field. In this case, the conversion rate cannot be increased by enhancing the mixing performance. In contrast, if the reaction is fast compared to mixing, the mixing rate can affect the conversion rate. The reaction takes place in a heterogeneous concentration field with multilamellae structures which are determined by the mixing process. The length scales of these structures as well as the time scale of their generation can have a strong influence on the conversion rate. In the case of a reaction system with competitive parallel or consecutive reactions, mixing time can also affect the selectivity of this system, especially if parallel reactions proceed at a different time scale.

This dependency can also be used for an application-oriented characterization of the mixing time by defined reaction systems. Several test reactions based on two competitive chemical reactions are described in the literature. They can be divided into two simplified schemes: The competitive parallel reaction system (Scheme 1) and the competitive consecutive reaction system (Scheme 2).

Scheme 1. Competitive Parallel Reaction System

$A + B \xrightarrow{k_1} R$	quasi-instantaneous
$C + B \xrightarrow{k_2} S$	fast

Scheme 2. Competitive Consecutive Reaction System

$A + B \xrightarrow{k_1} R$	quasi-instantaneous
$R + B \xrightarrow{k_2} S$	fast

The influence of the two previously mentioned reaction-to-mixing time ratios on the two reaction schemes is illustrated in Figures 1 and 2. The homogeneous condition (a) can be achieved only if mixing time t_m is short relative to the reaction time t_R of the slower reaction. In this case, the selectivity is only determined by the chemical kinetics. Since the rate constant k_1

Received: April 30, 2012
Published: August 15, 2012

   dx.doi.org/10.1021/op300107z | *Org. Process Res. Dev.* 2012, 16, 1513−1522

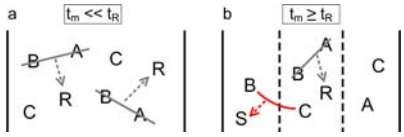

Figure 1. Competitive parallel reactions in a homogeneous (a) and a heterogeneous concentration field (b).

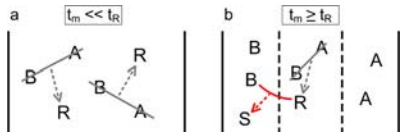

Figure 2. Competitive consecutive reactions in a homogeneous (a) and a heterogeneous concentration field (b).

is much larger than the rate constant k_2, the yield of product S (Y_S) approaches zero. In contrast, if the mixing time t_m is comparable to or longer than the reaction time t_R of the slower reaction (b), the reaction takes place at the interfacial region of the segregated fluid lamellae. After the immediate reaction of A and B, this region now contains an excess of species C. Subsequently, reactant C continues to diffuse toward the region with a local overconcentration of reactant B, where (in the absence of species A) the slower reaction can proceed. As a result, a detectable yield of product S will be achieved, depending on the degree of segregation.

A very commonly used competitive parallel reaction system is the iodide iodate reaction method known as the Villermaux–Dushman reaction.[2] This reaction system is simple to implement in the laboratory, but it is also associated with some difficulties, as reported by Falk[3] and Kölbl.[4] Several other test reactions have been developed by Baldyga, Bourne, and co-workers.[5−7] Two of them were used for the investigations described in the present paper: (1) neutralization and acetal hydrolysis, a system of fast competitive parallel reactions;[6] (2) diazo coupling between 1-naphthol and diazotized sulphanilic acid, a system of competitive consecutive reactions.[7]

In order to investigate micromixing phenomena at different time scales, the main criterion for the choice of the test reactions was the significant difference between the characteristic times for the slower reaction of each system. With suitable reactant concentrations, acetal hydrolysis takes place on the time scale of only a few milliseconds, while the time needed for the secondary azo coupling is about 2 orders of magnitude longer. Furthermore, practical reasons led to the choice of the two systems: The reaction mechanisms are fully investigated, and kinetic data are available in the literature.

Table 1. Investigated Micromixers

Investigated Micromixer Supplier		Mixing Principle and mixer dimensions
Slit interdigital micromixer SIMM-V2-ss Institut für Mikrotechnik Mainz GmbH, Mainz, Germany	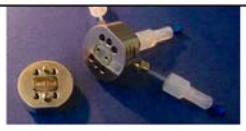	**Multilamination** Channels: 40 µm width, 200 µm depth Internal volume: approx. 8 µl
Caterpillar mixer CPMM-R150 Institut für Mikrotechnik Mainz GmbH, Mainz, Germany	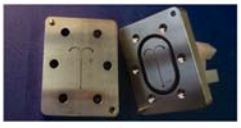	**Split-and-recombine** Mixing channel: 150 µm × 150 µm Internal volume: approx. 5 µl
X-mixer (type X) LTF-MX Little Things Factory GmbH, Ilmenau, Germany		**Mixing by repeated level change and crossflow** Internal Volume: approx. 200 µl
Chicane mixer (type S) LTF-MS Little Things Factory GmbH, Ilmenau, Germany		**Enhancement of mixing by flow obstacles** Internal Volume: approx. 200 µl
Separator mixer (type ST) HTM-ST-2-1 Little Things Factory GmbH, Ilmenau, Germany		**Enhancement of mixing by varying obstacles** Internal Volume: approx. 120 µl
T-Mixer, Y-Mixer Arrowhead-Mixer Upchurch Scientific, Oak Harbor, USA		**Simple contacting** *T-mixer:* Internal diameter: 1.25 mm Internal volume: approx. 18 µl *T-/Y-/Arrowhead-mixer:* Internal diameter: 0.5 mm Internal volume: approx. 3 µl
Static Mixing Tee (Arrowhead) Upchurch Scientific, Oak Harbor, USA		**10µm UHMW-PE frit in the mixing channel** Internal diameter: 0.5 mm Internal volume: approx. 3 µl

dx.doi.org/10.1021/op300107z | *Org. Process Res. Dev.* 2012, 16, 1513−1522

Different mixer types were investigated representing the most common mixing principles (Table 1). The different mixing structures can be divided into four groups of commonly used micromixers: (1) T-, Y-, and arrowhead configurations; (2) flow obstacles and chicanes within microchannels; (3) repeated flow split and recombination structures; (4) multi-lamination mixing principle.

EXPERIMENTAL SECTION

Experimental Setup. Since syringe pumps can provide accurate flows with very low pulsation, they are well suited to employ micromixers at typical flow rates and moderate pressures. Two precision syringe dosers (SyrDos 2, HiTec Zang) were used to obtain continuous flows, each one equipped with two pumps and 10 mL syringes. With an automated sample collector (AutoSam, HiTec Zang), samples were taken at different total flow rates in the range 0.5−50 mL/min. For pressure measurements, two piezoresistive pressure transmitters (model S-10, WIKA) were used. At the mixer outlet, a tube with an inner diameter of 1.58 mm and a length of 3 m was connected to ensure a sufficiently long residence time. Otherwise, in the case of poor mixing performance, the reaction may not be completed before the solution enters the sample vial.

Diazo Coupling. The principle of the competitive consecutive reaction system has been described previously in a simplified form (Scheme 2). The system developed by the team of J. R. Bourne is more complex, since it contains two primary couplings (eqs 1a and 1b) in which isomeric monoazo dyes (p-R and o-R) are formed. Subsequently, their secondary couplings (eqs 1c and 1d) produce one bisazo dye (S).

$$\mathrm{A} + \mathrm{B} \xrightarrow{k_{1o}} \text{o-R} \tag{1a}$$

$$\mathrm{A} + \mathrm{B} \xrightarrow{k_{1p}} \text{p-R} \tag{1b}$$

$$\text{o-R} + \mathrm{B} \xrightarrow{k_{2o}} \mathrm{S} \tag{1c}$$

$$\text{p-R} + \mathrm{B} \xrightarrow{k_{2p}} \mathrm{S} \tag{1d}$$

For the reaction scheme and especially kinetic aspects, see Baldyga[5] and Bourne.[7] The rate constants are given for a temperature of 298 K, pH = 9.9, and an ionic strength μ = 444.4 mol/m^3:

$$k_{1p} = 12238 \pm 446\ \mathrm{m^3/(mol\,s)}$$

$$k_{1o} = 921 \pm 31\ \mathrm{m^3/(mol\,s)}$$

$$k_{2p} = 22.25 \pm 0.25\ \mathrm{m^3/(mol\,s)}$$

$$k_{2o} = 1.835 \pm 0.018\ \mathrm{m^3/(mol\,s)}$$

The limiting reagent in the system is the diazotized sulphanilic acid (B), since it is consumed by all reactions. When the reactions are completed, a determination of the product concentrations enables calculation of the selectivity of the comparatively slower secondary couplings. Based on a fitting material balance and no further byproduct formation, the yield of the bisazo dye S in relation to the initial concentration of B (c_{B0}) can be defined as

$$Y_S = \frac{2c_S}{c_{B0}} = \frac{2c_S}{c_{oR} + c_{pR} + 2c_S} \tag{2}$$

where c_{oR}, c_{pR}, and c_S are the concentrations of the products o-R, p-R, and S (see Table 2). The initial solution containing the diazonium salt was prepared by diazotization of 3 mol/m^3 sulphanilic acid with sodium nitrite and hydrochloric acid. Excess nitrite was eliminated by adding sulphamic acid. 3.6 mol/m^3 of 1-naphthol was dissolved in water by stirring and heating the solution. This stream was buffered using 222.2 mol/m^3 each of sodium carbonate and bicarbonate in order to obtain a pH of 9.9 and an ionic strength μ = 444.4 mol/m^3 in the mixed product solution. Due to the limited stability of the reactants, both solutions were prepared directly before starting the experiments.

Table 2. Symbols and Names of Reagents in Eqs 1a−1d

symbol	name
A	1-naphthol
B	diazotized sulphanilic acid
o-R	2-[(4′-sulphophenyl)azo]-1-naphthol
p-R	4-[(4′-sulphophenyl)azo]-1-naphthol
S	2,4-bis[(4′-sulphophenyl)azo]-1-naphthol

After collecting the samples, the product mixture was diluted with buffer solution. The absorption of each sample was measured at a wavelength range of 400−700 nm. In order to determine the concentration of the different dyes, multilinear regression analysis was performed for the measured absorption spectra. The calculations with multilinear spectra are based on the molar extinction coefficients for each single substance (Figure 3) given by Bourne and co-workers.[7] Since the absorption spectra of the monoazo dyes are very similar, their concentrations were determined in sum (c_{oR} + c_{pR}).

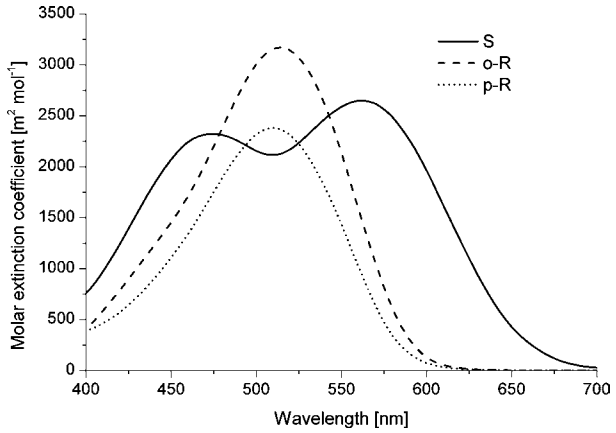

Figure 3. Molar extinction coefficients for the bisazo dye (S) and both monoazo dyes (o-R, p-R), for μ = 444.4 mol/m^3 and T = 298 K.

For each measurement, a mass balance check was carried out by comparing the initial amount of diazotized sulphanilic acid with the amount of the azo dyes in the product solution. It was found that the mass balance closes very well (±5%) for low values of Y_S. For higher yields (>20%), a significant amount of B is apparently not converted to any of the three dyes, which indicates the formation of unidentified byproducts.[5] Since the deviation in the mass balance is systematic and increases with

dx.doi.org/10.1021/op300107z | Org. Process Res. Dev. 2012, 16, 1513−1522

increasing values of Y_S, the qualitative conclusions about the mixing performance are still valid.

DMP Hydrolysis. The competitive parallel reaction scheme, containing a neutralization reaction and an acetal hydrolysis, was studied by Baldyga, Bourne, and co-workers. A detailed thermochemical and kinetical characterization of this system can be found in publications of Baldyga et al.[5,6] and Lindenberg.[8] In the experiments, a solution of sodium hydroxide and 2,2-dimethoxypropane (DMP) is mixed with an acid solution:

$$H^+ + OH^- \xrightarrow{k_1} H_2O \tag{3}$$

$$H^+ + CH_3C(OCH_3)_2CH_3 + H_2O \xrightarrow{k_2} H^+ + CH_3COCH_3 + 2CH_3OH \tag{4}$$

With a second-order rate constant $k_1 = 1.4 \times 10^8$ m^3 mol^{-1} s^{-1}, the neutralization of sodium hydroxide is very fast and can be considered as quasi-instantaneous. By comparison, the formation of acetone and methanol in the acid catalyzed hydrolysis of DMP is significantly slower. Due to the high excess of water, the reaction rate can be simplified to second order with a rate constant k_2 given in m^3 mol^{-1} s^{-1}:

$$k_2 = 7.32 \times 10^7 \exp(-5556/T) 10^{(0.05434+7.07\times10^{-5}c_S)} \tag{5}$$

This relation was determined by Baldyga et al.[6] for a temperature range of 298−313 K, acid and DMP concentrations of 25−1333 mol/m^3, and an ethanol concentration of 25 wt %. Since increasing salt concentrations accelerate hydrolysis, the expression additionally contains the sodium chloride concentration c_S and is valid for a range of 100−1200 mol/m^3.

As soon as all acid molecules are neutralized, the reaction process is completed and the conversion X_{DMP} of the slower reaction can be determined to characterize mixing:

$$X_{DMP} = 1 - \frac{c_{DMP}}{c_{DMP,0}} \tag{6}$$

Here, c_{DMP} is the concentration of DMP in the final product solution after mixing and reaction while $c_{DMP,0}$ is the concentration in the perfectly mixed product solution for the theoretical case that no conversion of DMP occurred. The conversion of DMP can be considered as an average result of fluid segregation during the reaction process.

Both initial solutions contained 25 wt % ethanol in deionized water and 90 mmol/L NaCl. It must be noted that contrary to the system described by Baldyga et al., nitric acid was used instead of hydrochloric acid. Thus, corrosion in the stainless steel micromixers should be avoided. Due to the formation of $NaNO_3$, deviations from the rate constant described by eq 5 are possible. However, a comparison between experiments with both acids did not show a significant difference in the results.

One solution with 600 mol/m^3 HNO_3 was prepared, and a second solution contained 600 mol/m^3 DMP and 630 mol/m^3 NaOH. The 5% excess of NaOH assures a pH larger than 8 in the mixed solution in order to avoid further reaction of DMP. Within a time of 24 h after the experiments, no further decomposition of DMP was observed. Anyway, all samples were analyzed immediately after collection on a HP 5890 gas chromatograph equipped with a 30 m Quadrex column (#007-5-30-0.25F) and a flame ionization detector. A split injection with an injection volume of 0.2 μL provided the best results. The oven temperature of 60 °C was kept constant for 1 min and then increased to 140 °C with a ramp of 10 °C/min.

RESULTS AND DISCUSSION

Reaction Time and Mixing Time. In order to determine the characteristic reaction times, the case of an approximately homogeneous concentration field is assumed. Thus, the half-life of species B in a second order reaction can be expressed as

$$t_{1/2} = \frac{1}{k_2 c_{B0}} \tag{7}$$

With the chosen concentrations and kinetic data for a temperature of 298 K (see Experimental Section), a half-life of about 5 ms results for DMP hydrolysis. Due to the more complex reaction scheme of the diazo coupling with several parallel and consecutive reactions, further simplifications are made for this system: Since k_{1o} is small relative to k_{1p}, the reaction path via the monoazo dye o-R (see eq 1) can be neglected. The half-life is determined for a state of reaction when half of the diazotized sulphanilic acid already reacted with the monoazo dye p-R. Therefore, the resulting time of 727 ms can only be considered as a rough estimation for the time frame of the reaction. Furthermore, if the chemical reaction proceeds in the time frame of mixing, it takes place in a heterogeneous concentration field with unequal molar ratios. Due to the spatial differences in concentration, a local chemical reaction rate exists for each region.

In order to compare these reaction times with regard to the mixing process, diffusion time has to be considered. Molecular diffusion is always required as a final step when it comes to mixing reactants on a molecular scale. According to Falk and Commenge,[9] diffusion time can be expressed as

$$t_{diff} = A\frac{R^2}{D} \tag{8}$$

D is the diffusion coefficient while R denotes the half length scale of the aggregate. The shape factor A integrates the shape of the flow structure. It is defined by

$$A = \frac{1}{(p+1)(p+3)} \tag{9}$$

including a shape parameter p (slab, $p = 0$; cylinder, $p = 1$; sphere, $p = 2$). In a plane multilamellae flow pattern, $p = 0$ can be used to calculate diffusion in micromixers. The shape parameter $p = 1$ can be used to describe tubes with concentric flow patterns (for a practical setup, see ref 10). In most cases, the structures are deformed, for example by laminar vortices, so that the shape parameter can only be used for a simplified evaluation of mixing time. The investigated micromixer with the finest structures is the slit interdigital micromixer (SIMM). The inlet of this mixer generates a 40 μm multilamellae flow which is focused to 15.6 μm slab size in a following narrow bore.[11] According to eq 8, for a slab in water ($D \approx 10^{-9}$ m^2 s^{-1}) a diffusion time of approximately 80 ms results. Additional mixing effects due to the sudden changes of the diameter in the mixing element are neglected for this consideration. The comparison with the reaction time of the DMP hydrolysis above shows that, even at this small length scale, mixing only based on diffusion is not significantly faster than the half-life of the reactant. To achieve diffusion times even shorter than the time for DMP hydrolysis, slab sizes have to be reduced by at least 1 order of magnitude. A possible way to increase the

dx.doi.org/10.1021/op300107z | Org. Process Res. Dev. 2012, 16, 1513−1522

mixing performance in the SIMM after the establishment of the laminar fluid structure is to focus further the initial structure with a stronger narrowing mixing channel.[11] However, in most micromixers, only one interface exists after contacting the reactant flows. Mixing performance is here mainly based on the formation of vortices (an example of which is illustrated in Figure 4) which create fine structures with length scales of only a few micrometers.[12] Concentration differences on these scales can be eliminated very fast by diffusion.

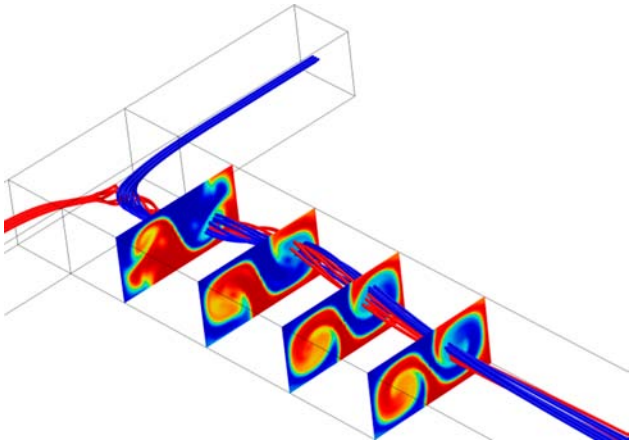

Figure 4. CFD simulation (COMSOL Multiphysics) of the vortex formation in a T-mixer. The planes depict the concentration profiles in the mixing channel (size, 1 mm × 2 mm; total flow rate, 16.8 mL/min).

The influence of the different time scales of reaction in the two test reaction systems is shown in Figure 5 using T-mixers with different inner diameters as an example.

In the experiments with the diazo coupling test system, the yield of the bisazo dye Y_S decreases, indicating an enhancement of mixing performance in the range between 0 and 24 mL/min. The faster mixing occurs, the less time is available for the slower formation of the bisazo dye. Due to the increasing flow rate, the improved vortex formation causes a reduction of mixing time. At a total flow rate above 20 mL/min, mixing time is short enough to approach fully homogeneous conditions for the reaction and the formation of the bisazo dye cannot take place. Therefore, at these flow rates, the yield Y_S is close to zero.

As shown above, the reaction time of DMP hydrolysis is about 2 orders of magnitude shorter. Hence, for a decrease of the DMP conversion X_{DMP}, much shorter mixing times are required. With a simple T-mixer, such rapid mixing is only possible at high flow rates above 20 mL/min. However, even at a throughput of 48 mL/min, the mixing performance is still not sufficient to reach DMP conversions close to zero.

At flow rates below 15 mL/min, a slight increase in the value of X_{DMP} can be observed. A possible explanation is based on the change of the residence time in the short and narrow mixing channel. Both mixers were connected to a capillary with a larger internal diameter of 1.58 mm. This fact is important if a strict laminar flow without vortex formation is assumed for low volume flows. In this case, molecular diffusion is the main driving force for the mixing process. As can be seen from eq 8, the mixing time for diffusion correlates with the characteristic length scale by a quadratic dependence. Therefore, the sudden enlargement of the channel diameter at the outlet of the T-mixer has an important influence. Since diffusion time is significantly longer in the connected capillary, mixing time is mainly influenced by the actual narrow mixing channel of the T-piece. Increasing the flow rate leads to a decrease in the available time for diffusive mass transfer in this segment. Thus, the mixing performance decreases with the residence time in the T-mixer, until at higher flow rates vortex formation predominates as a main driving force for mixing.

In order to prove the suitability of the chosen reaction systems to classify different mixers by their mixing performance, T-mixers with different internal diameters were used for a comparison. For equal volume flow rates, the flow velocity is higher in the smaller mixing channel. Therefore, more intense vortex formation and thus shorter mixing times have to be assumed. Vortex formation can take place in the T-piece as well as in the transition to the connected tube due to the sudden enlargement of the diameter. It has to be considered that the two mixer set-ups are not geometrically similar, since the relative increase of the internal diameter is much stronger for the T-mixer with an internal diameter of 0.5 mm.

For both reaction systems, the prediction of faster mixing at the smaller channel diameter can be confirmed. As can be seen in Figure 5, the decrease of the values of Y_S and X_{DMP}, respectively, starts at lower total flow rates for the mixer with an internal diameter of 0.5 mm compared to the mixer with an internal diameter of 1.25 mm. For the hydrolysis of DMP, at higher flow rates the DMP conversion is significantly lower when using the T-mixer with a channel diameter of 0.5 mm.

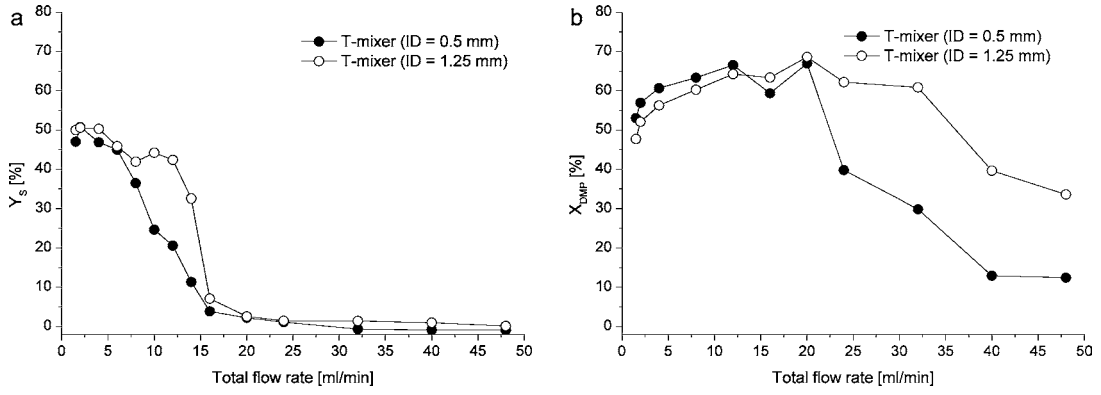

Figure 5. Comparison of the experimental results of T-mixers with different inner diameters for the azo coupling test reaction (a) and DMP hydrolysis (b).

dx.doi.org/10.1021/op300107z | Org. Process Res. Dev. 2012, 16, 1513–1522

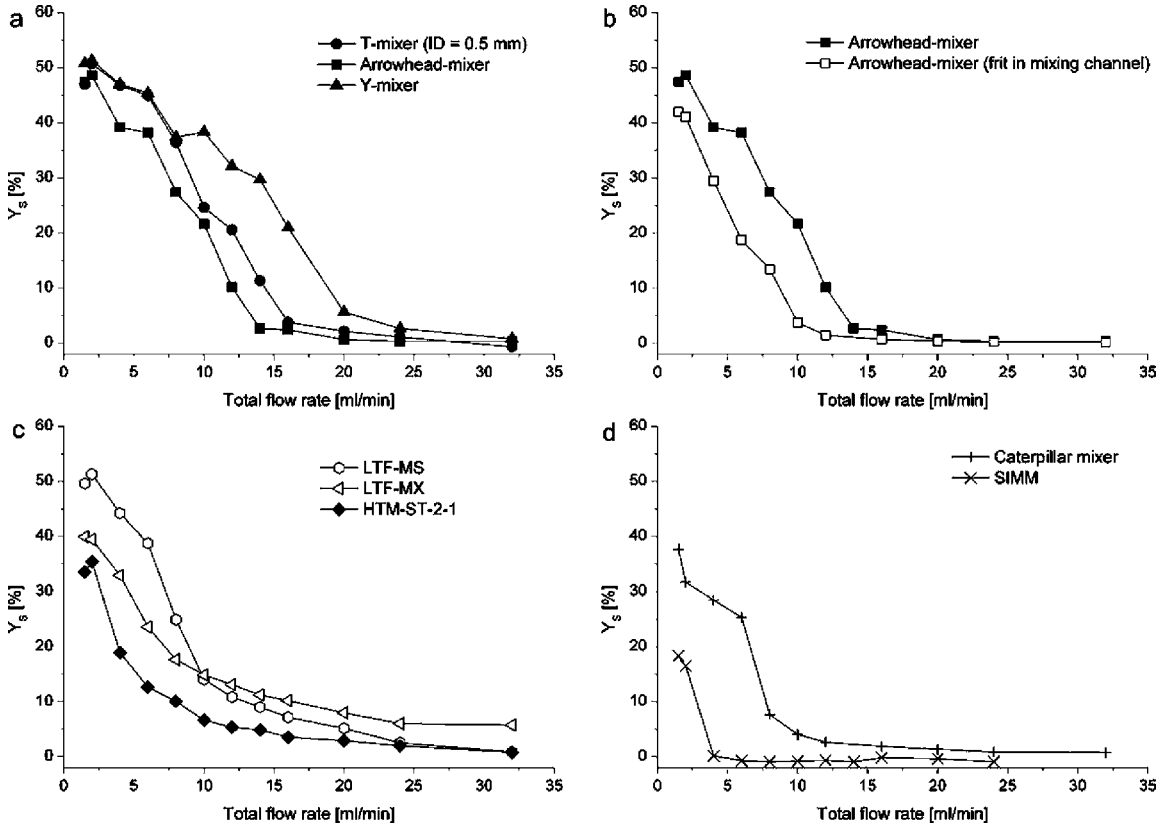

Figure 6. Experimental results of the bisazo dye yield Y_S as a function of the total flow rate for all investigated micromixers.

In conclusion, the combination of both test reactions allows an estimation of the mixing performance over a large investigated flow range (0−48 mL/min). The example of the two T-mixers shows that mixing time can be shortened continuously by increasing the total flow rate.

Diazo Coupling Test Reaction. In Figure 6 the results for the diazo coupling test reaction are shown sorted by vendor. For some mixers, slightly negative values for the bisazo dye yield occur. They can be attributed to the error in conjunction with the multilinear regression analysis to determine the product concentrations out of the absorbance spectra.

Figure 6a shows the comparison between types of T-pieces with alternative arrangements of the feed and mixing channels. For all flow rates, the lowest values of Y_S can be reached with the arrowhead geometry while the Y-mixer shows the worst mixing performance. In the Y-mixer a lower energy dissipation is caused by the minor redirection of the flow. As a result, especially at high flow rates, the values for Y_S are considerably higher compared with those for the T-mixer. In contrast, the mixer with arrowhead geometry seems to provide slightly shorter mixing times. This is caused by a higher local energy input due to the sharper angle between the feed and mixing channels.

The investigation of the arrowhead mixer containing a frit in the mixing channel (Figure 6b) showed considerable low bisazo dye yields. By comparing the results with an arrowhead mixer of similar geometry, it is obvious that the frit with a pore size of 10 μm has an accelerating effect onto the mixing rate. Although an improved mixing performance was to be expected, the extent of the increase in efficiency is remarkable.

The micromixers designed by the Institut für Mikrotechnik Mainz (results in Figure 6d) stand out due to their very small dimensions of the mixing channels. In particular, the SIMM shows excellent mixing performance for the competitive diazo coupling in the entire throughput range. The value of Y_S tends to zero at a flow rate of only 6 mL/min. In order to reach a comparable mixing performance with the caterpillar mixer, a significantly higher flow rate of at least 16 mL/min is necessary. The superior performance of the SIMM can be explained by the fact that in the SIMM, after contacting the reactant solutions, instantaneously a multilamellae structure exists. In combination with focusing and the formation of vortices at higher flow rates in the further mixing channel, mixing at a molecular scale can be completed in a very short time. In contrast, the split and recombine mixing principle of the caterpillar mixer is based on a successive halving of lamellae width throughout the entire mixing channel. At the beginning of the mixing channel, the fluids are more segregated. Hence, in this region, the slower secondary azo coupling is able to proceed.

In Figure 6c the three different glass mixers (Little Things Factory GmbH) are compared. It is noticeable that, at flow rates up to about 10 mL/min, the slope of the curve is steeper than that at higher flow rates. The most effective glass mixer for this reaction system seems to be the HTM-STM-2-1 mixer; a considerably poorer mixing performance can be observed for the LTF-MS and LTF-MX. In these mixers, mixing takes place in a comparatively large reactor volume at mixing channel widths of about 1 mm and a length of approximately 10 cm. The residence time in the mixer is significantly longer compared to those for the other investigated mixers. If the total flow rate is high enough to induce intensive vortex formation, it can be assumed that the mixing time is shorter than the residence time in the mixer. Therefore, the mixing

dx.doi.org/10.1021/op300107z | Org. Process Res. Dev. 2012, 16, 1513−1522

efficiency in only the front part of the mixing channel would be determined. This assumption is confirmed by the view of the visible mixing state in the glass mixers. As an example, in Figure 7 the progressive formation of the azo dyes in the LTF-MS mixing channel is shown for a total flow rate of (a) 8 mL/min and (b) 16 mL/min.

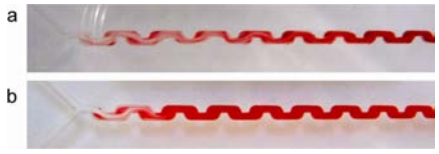

Figure 7. Pictures of the fluid dyeing in the mixing channel of the LTF-MS mixer for a total flow rate of 8 mL/min (a) and 16 mL/min (b).

At the higher flow rate, a uniform coloring of the fluid is observed shortly after the entrance into the mixing channel even though the residence time in the whole mixing channel is shorter. This indicates that the improvement of mixing by increasing the flow rate outweighs the reduction of the residence time.

However, the HTM-ST-2-1 mixer performed very well compared to the other mixers of Little Things Factory GmbH. The LTF-MX, on the other hand, was the only mixer unable to reach yields lower than 5% even at higher flow rates. A possible explanation is the mixing principle, which is based on the repeated change of the two levels of the mixer. The mixing quality increases with the number of mixing elements. Hence, this procedure cause a good mixing quality at the end of the mixer, but due to the high inner volume of the mixer, it processes too slowly to avoid the secondary azo coupling completely.

DMP Hydrolysis Test Reaction. The comparison between the T-mixer, the Y-mixer, and the arrowhead mixer (Figure 8a) shows effects that are similar to those at the azo coupling test reaction. However, although the performance of the Y-mixer again is poorer compared to the case of the T-mixer at high flow rates, no observable difference can be seen between the T- and the arrowhead geometry. Here again, the frit as an additional mixing element causes a significant enhancement of the mixing performance (see Figure 8b). It must be noted that the curves in Figure 8 are shown for a different range of flow rates compared to the case of Figure 6. A decrease of the DMP conversion occurs at significantly higher flow rates.

The fast decrease of the DMP conversion in the curve of the SIMM (Figure 8d) indicates a superior mixing performance of this mixer, which is consistent with the results of the diazo coupling experiments. It is the only investigated micromixer in which DMP conversion could be avoided completely. However, a minimum total flow rate of about 8 mL/min is necessary to reach this performance. At lower flow rates, approximately pure laminar flow resulting in a bad mixing performance can be assumed.

The above-mentioned disadvantages of the caterpillar mixer compared to the SIMM can also be observed using the DMP hydrolysis reaction system. As a result of the successive scaling down of lamellae width throughout the mixing channel, a homogeneous concentration field cannot be created as fast as in

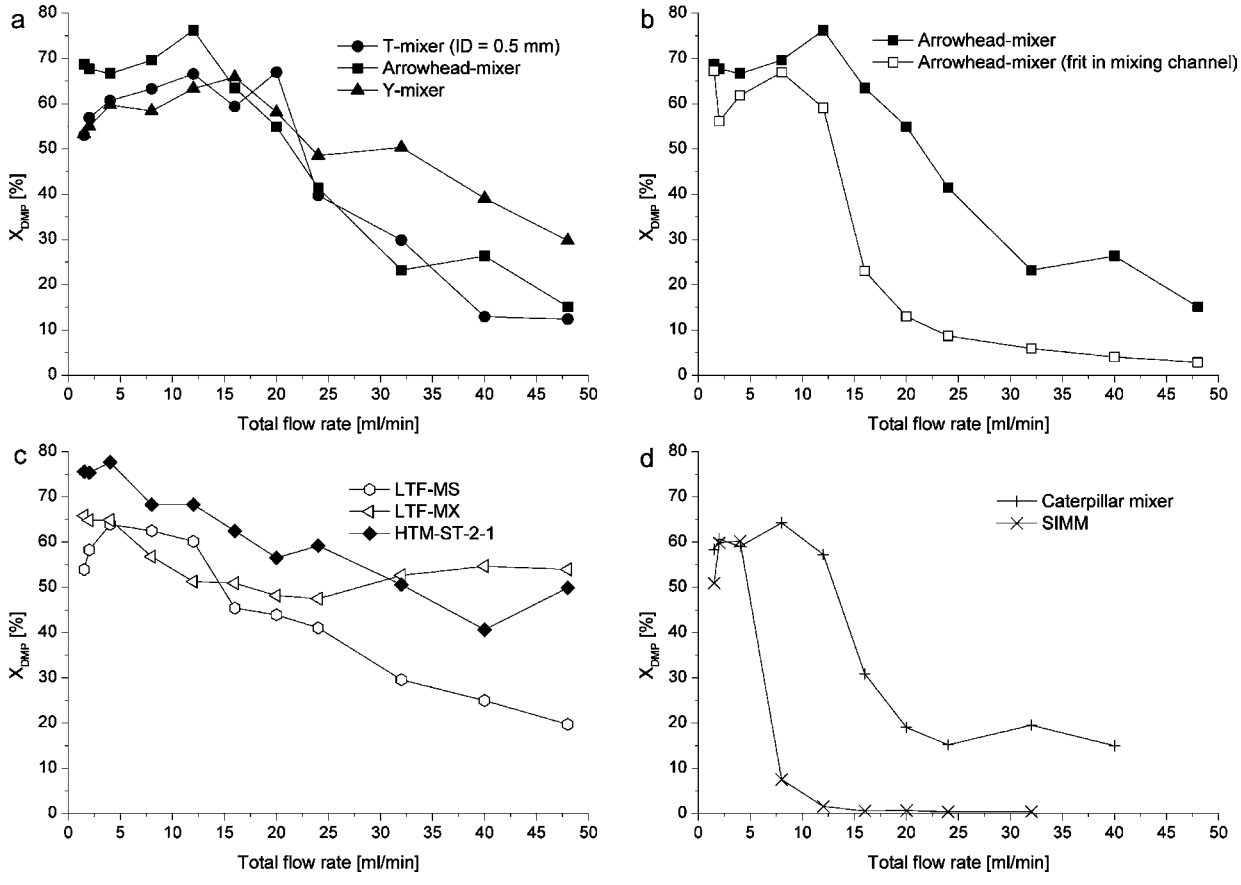

Figure 8. Experimental results of the DMP conversion X_{DMP} as a function of the total flow rate for all investigated micromixers.

dx.doi.org/10.1021/op300107z | Org. Process Res. Dev. 2012, 16, 1513−1522

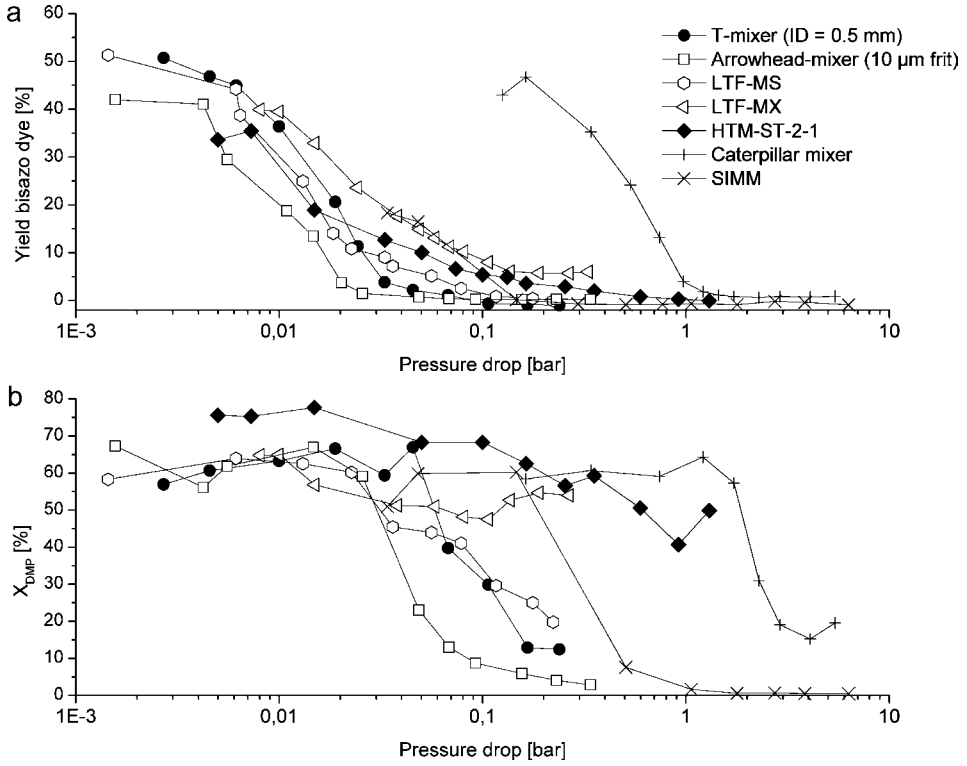

Figure 9. Results of the DMP hydrolysis test system (a) and diazo coupling test system (b) with regard to the measured pressure drop for comparable flow rates. For each micromixer, the pressure drop was determined at the same flow rates that are shown in Figures 6 and 8.

the SIMM. Since DMP conversion proceeds in only a few milliseconds, a considerable influence on X_{DMP} results. According to the curve in Figure 8d, a DMP conversion of 15% seems to be a minimum value in the investigated volume flow range.

The curves in Figure 8c suggest that the investigated glass mixers do not mix fast enough to suppress the DMP hydrolysis. This observation makes sense, since even at the highest flow rate, the residence time would be longer than 200 ms. For a low DMP conversion, mixing on the molecular scale would have to be completed after a few milliseconds, in the first millimeters of the mixing channel. Further mixing elements do not have any influence on the DMP conversion. Therefore, mixers with dimensions in the range of 1 mm are inefficient if mixing times in the range of DMP hydrolysis are required.

Mixing Performance and Pressure Drop. For the evaluation of the mixing efficiency of a micromixer, the required energy input of the mixing process has to be taken into account. The pressure drop of a micromixer is directly related to the energy input. Ideally, most of the energy input is used effectively for mixing. In contrast, a poorly constructed micromixer shows a high pressure drop without using this energy input for the mixing process. Therefore, the results of both test reaction systems have to be discussed in terms of the measured pressure drops (Figure 9). An efficient mixer provides a certain mixing time short enough for a specific application by causing a low pressure drop. To give an example, the results of the caterpillar mixer and the arrowhead mixer with a frit in the mixing channel indicate similar mixing performance for both test reactions (see Figures 6 and 8). However, with regard to the pressure drop, the values differ by nearly 2 orders of magnitude, as shown in Figure 9. While the pressure drop caused by the short frit (10 μm pore size) in the mixing channel of the arrowhead mixer (i.d. = 0.5 mm) is comparatively moderate, the 150 μm structured mixing channel of the caterpillar mixer gives a very high loss of pressure even at low flow rates. Thus, for both reaction systems, the caterpillar mixer seems to be less energy efficient.

Due to the fine structures of the SIMM inlet, the pressure drop in the upper range of flow rate is even higher in the SIMM compared to the caterpillar mixer. Since the SIMM performs very well even at low flow rates, nevertheless, short mixing times can be achieved with moderate pressure drop at limited throughput.

In both parts a and b of Figure 9, similarities between the curves of the T-mixer and the LTF-MS mixer can be identified. Only in these mixers, no splitting of the flow by the mixer structure takes place. Thus, fast mixing can only be reached by the formation of vortices in the mixing channel. It can be assumed that the extent of the vortex formation correlates with the energy input and the pressure drop, respectively.

As indicated by the significant differences of the curves in both figures, not only the energy input but also the dimensions and the mixing principle seem to have a great influence on the mixing performance. In some mixers, for certain volume flows, mixing may be already completed in the front part of the mixing channel (e.g., LTF-MS). Therefore, only part of the energy input is effectively used for mixing. The measured pressure drop is higher than the actual pressure drop needed to achieve a certain mixing level. Especially for the glass mixers with comparably high inner volumes, this effect may lead to an underestimation of the mixing efficiency.

Micromixer Selection and Scale-up. The investigations presented in this paper focus on the efficiency of micromixers. In order to select a commercially available micromixer for a mixing sensitive reaction, the following procedure is proposed:

Table 3. Colored Representation of the Mixing Performance Based on the Yield of Bisazo Dye Y_S Using the Diazo Coupling Test Reaction ($t_{1/2} \approx 730$ ms)[a]

Micromixer	Y_S [-]	Total flow rate [ml/min]										
		1	2	4	8	12	16	20	24	32	40	48
T-mixer (d = 1,25 mm)		50.0	50.6	50.3	41.9	42.4	7.1	2.5	1.5	1.4	1.0	0.1
T-mixer (d = 0,5 mm)		47.0	50.8	46.9	36.4	20.6	3.8	2.2	1.1	-0.6	-0.9	-1.0
LTF-MS		49.6	51.3	44.2	24.9	10.9	7.2	5.2	2.5	0.8	0.5	0.0
LTF-MX		39.9	39.5	32.9	17.6	13.1	10.2	8.0	6.0	5.7	5.7	6.0
Caterpillar mixer		43.0	46.8	35.2	13.2	1.9	0.9	0.6	0.9	0.8	0.9	
Arrowhead-mixer (10 µm frit)		42.0	41.1	29.5	13.5	1.5	0.7	0.4	0.2	0.2	0.3	0.2
HTM-ST-2-1		33.6	35.4	18.9	10.1	5.4	3.6	2.9	2.0	0.8	0.3	0.0
Slit interdigital micromixer		18.3	16.5	0.2	-0.9	-0.6	-0.9	-0.2	-0.4	-0.9		

[a]Green, best performance; red, poorest performance. Negative values can be attributed to the error in conjunction with the multilinear regression analysis to determine the product concentrations out of the absorbance spectra (see Experimental Section).

Table 4. Colored Representation of the Mixing Performance Based on the DMP Conversion X_{DMP} Using the DMP Hydrolysis Test Reaction ($t_{1/2} \approx 5$ ms)[a]

Micromixer	X_{DMP} [-]	Total flow rate [ml/min]										
		1	2	4	8	12	16	20	24	32	40	48
LTF-MX		65.8	64.8	64.9	56.8	51.3	50.9	48.2	47.5	52.7	54.7	54.0
HTM-ST-2-1		75.6	75.3	77.7	68.3	68.3	62.5	56.5	59.2	50.6	40.7	49.9
T-mixer (d = 1,25 mm)		47.7	52.1	56.2	60.2	64.3	63.4	68.6	62.2	60.8	39.6	33.5
T-mixer (d = 0,5 mm)		53.0	57.0	60.7	63.3	66.6	59.4	67.0	39.8	29.9	12.9	12.4
LTF-MS		53.9	58.3	63.9	62.5	60.2	45.5	43.9	41.1	29.6	25.0	19.8
Caterpillar mixer		58.4	60.7	59.1	64.3	57.3	30.9	19.0	15.2	19.5	15.0	
Arrowhead-mixer (10 µm frit)		67.3	56.1	61.8	66.9	59.1	23.0	13.0	8.7	5.9	4.0	2.8
Slit interdigital micromixer		51.0	59.9	60.2	7.6	1.6	0.6	0.7	0.5	0.5		

[a]Green, best performance; red, poorest performance.

Table 5. Colored Representation of the Pressure Drop Δp of the Investigated Micromixers (Values in bar)[a]

Micromixer	Δp [bar]	Total flow rate [mL/min]										
		1	2	4	8	12	16	20	24	32	40	48
HTM-ST-2-1		0.005	0.007	0.015	0.050	0.100	0.164	0.255	0.354	0.596	0.920	1.302
T-mixer (d = 1,25 mm)		0.026	0.037	0.079	0.158	0.240	0.325	0.410	0.498	0.680	0.871	1.105
T-mixer (d = 0,5 mm)		0.043	0.052	0.094	0.178	0.261	0.359	0.452	0.560	0.782	1.022	1.283
LTF-MS		0.035	0.065	0.097	0.188	0.283	0.373	0.481	0.597	0.829	1.085	1.366
Arrowhead-mixer (10 µm frit)		0.034	0.046	0.092	0.190	0.288	0.398	0.513	0.630	0.906	1.204	1.548
LTF-MX		0.066	0.082	0.108	0.215	0.328	0.441	0.551	0.683	0.940	1.224	1.524
Caterpillar mixer		0.212	0.287	0.583	1.215	1.904	2.588	3.344	4.050	5.711	6.541	
Slit interdigital micromixer		0.089	0.137	0.298	0.743	1.349	2.169	3.183	4.374	7.309		

[a]Green, lowest pressure drop; red, highest pressure drop.

First, it has to be considered if the reaction system is mixing-sensitive. As an experimental approach, the comparison of the product distribution resulting from mixing with two micromixers which strongly differ in their mixing performance could show this mixing sensitivity. Furthermore, an approximate time range that is required for mixing should be known. On that basis, either Table 3 ($t_{1/2} \approx 730$ ms) or Table 4 ($t_{1/2} \approx 5$ ms) can be used to find an appropriate mixer type. In combination with Table 5 (pressure drop), an overview is given to provide a scale-up strategy for the use of different micromixing devices: A scale-up to another micromixer can be considered to be assured if both mixers show similar behavior for the test reaction.

As an example, we assume a process that requires a mixing time in the range of only a few milliseconds. Therefore, the decision for the scale-up has to be based on the DMP reaction system. The process has been carried out successfully in the laboratory scale with a slit interdigital micromixer at a total flow rate of 10 mL/min. It is to be scaled-up to a significantly higher throughput of 50 mL/min. As can be seen in Table 5, the SIMM is not suitable for such a high flow rate, since a pressure drop higher than 7 bar would result. It is apparent from Table 4 that the arrowhead mixer including the short frit in the mixing channel is a good alternative in this range of mixing time. Furthermore, with a pressure drop of less than 2 bar at 48 mL/min, this mixer can be used with a moderate energy input.

For the case that a mixing time of about 1 s is sufficient for the process, Table 3 can be used to choose an appropriate mixer. At 50 mL/min, most of the investigated micromixers meet the requirements of the mixing performance. In this case,

dx.doi.org/10.1021/op300107z | Org. Process Res. Dev. 2012, 16, 1513−1522

a simple T-mixer would be the cheapest and most efficient choice.

It has to be emphasized that, in both cases, the overview Tables 3 and 4 only provide information about the ratio between mixing time and the particular reaction time. If mixing time does not affect the selectivity of a reaction system, slower mixing does not have to be a disadvantage as long as a homogeneous concentration field exists at the end of the mixing channel. In order to achieve this state, the mixing time has to be shorter than the residence time in the mixing device. Nevertheless, information about the range of mixing time is important for the choice of an effective reactor. As shown in the sections above, in the mixers with a large internal volume (e.g., LTF-MS), effective mixing takes place in only a small part of the mixing channel. Therefore, part of the energy input is used to mix a fluid with an already homogeneous concentration field.

In principle, the same scale-up concept as shown in this paper can be used for a scale-up to full-scale production. The mixing behavior at these significantly higher flow rates is an interesting topic for further investigations. A possible setup for this purpose could include static mixers,[13] the star laminator from the IMM,[14] or microreactors from Lonza.[15]

CONCLUSIONS

The mixing behavior of selected micromixers was experimentally characterized with two different competitive reaction systems. The systems differ in their reaction rate, which made it possible to evaluate the mixing performance of the different mixer types at two different time scales (~5 ms and ~730 ms). It has been shown that mixing times of only a few milliseconds can be achieved by using microstructured mixing channels. The investigated slit interdigital mixer exhibits superior mixing performance even at low flow rates. It was found that an arrowhead-mixer containing a short frit in the mixing channel shows a very effective mixing behavior. Mixing devices with structures in the range of a millimeter are suitable to achieve mixing times in the time range of the slower reaction system (>700 ms). Furthermore, it was shown that simple T-mixers can be used for very fast mixing if the energy input is sufficiently high. The influence of the energy input was studied by measuring the pressure drop of the mixers. Although pressure drop is a key parameter for mixing performance, the results indicate that mixing time is not exclusively determined by the overall energy input. It can be concluded that the mixing principle as well as the mixer design and geometry have an important influence on the effectiveness of a mixer.

The results that can be obtained by using test reaction systems always must be considered in context with the characteristic reaction time. An example scale-up consideration for the selection of an appropriate micromixer for mixing sensitive reactions based on the presented results is shown.

AUTHOR INFORMATION

Corresponding Author

*E-mail: t.roeder@hs-mannheim.de. Telephone: +49 621 292 6800.

Notes

The authors declare no competing financial interest.

ACKNOWLEDGMENTS

The authors would like to thank Novartis Pharma AG (CH-4002 Basel, Switzerland) and Land Baden-Württemberg for the financial support within the framework of the "MINT Projekt 2010".

REFERENCES

(1) For reviews on mixing principles, see: (a) Hessel, V.; Löwe, H.; Schönfeld, F. *Chem. Eng. Sci.* **2005**, *60*, 2479−2501. (b) Nguyen, N.; Wu, Z. *J. Micromech. Microeng.* **2005**, *15*, R1−R6.

(2) Guichardon, P.; Falk, L. *Chem. Eng. Sci.* **2000**, *55*, 4233−4243.

(3) Falk, L.; Commenge, J.-M. Characterization of Mixing and Segregation in Homogeneous Flow Systems. In *Micro Process Engineering: A Comprehensive Handbook*; Hessel, V., Renken, A., Schouten, J. C., Yoshida, J., Eds.; WILEY-VCH: 2009; Vol. *1*, pp 162−165.

(4) Kölbl, A. *Chem. Eng. J.* **2008**, *145*, 176−177.

(5) Baldyga, J.; Bourne, J. R. *Turbulent Mixing and Chemical Reactions*; John Wiley & Sons: Chichester, 1999.

(6) Baldyga, J.; Bourne, J. R.; Walker, B. *Can. J. Chem. Eng.* **1998**, *76*, 641−649.

(7) Bourne, J. R.; Kut, O. M.; Lenzner, J.; Maire, H. *Ind. Eng. Chem. Res.* **1990**, *29*, 1761−1765.

(8) Lindenberg, C.; Schöll, J.; Vicum, L.; Mazzotti, M.; Brozio, J. *Chem. Eng. Sci.* **2008**, *63*, 4135−4149.

(9) Falk, L.; Commenge, J.-M. *Chem. Eng. Sci.* **2010**, *65*, 405−411.

(10) Hassan, A. A.; Sandre, O.; Cabuil, V.; Tabeling, P. *Chem. Commun.* **2008**, *15*, 1783−1785.

(11) Hessel, V.; Hardt, S.; Löwe, H.; Schönfeld, F. *AIChE J.* **2003**, *49*, 566−577.

(12) Kockmann, N. *Transport Phenomena in Micro Process Engineering*; Springer-Verlag: 2007.

(13) Brechtelsbauer, C.; Ricard, F. *Org. Process Res. Dev.* **2001**, *5*, 646−651.

(14) Werner, B.; Hessel, V.; Löb, P. *Chem. Eng. Technol.* **2005**, *28*, 401−407.

(15) Kockmann, N.; Gottsponer, M.; Roberge, D. M. *Chem. Eng. J.* **2011**, *167*, 718−726.